Comparative Study on the Interaction of Scandium and Copper Atoms with Small Silicon Clusters

Chuanyun Xiao,* Ashley Abraham, Reginald Quinn, and Frank Hagelberg*

Computational Center for Molecular Structure and Interactions, Jackson State University, Jackson, Mississippi 39217

William A. Lester, Jr.

Kenneth S. Pitzer Center for Theoretical Chemistry, Department of Chemistry, University of California at Berkeley, Berkeley, California 94720-1460

Received: July 18, 2002

A comparative study of the interaction of M (M = Sc, Cu) atoms with small Si_n ($n = 1-6$) clusters is performed by means of a hybrid density functional technique (B3LYP) in conjunction with a 6-311+G(d) basis set. The structures identified for the most stable isomers of MSi_n are usually different for M = Sc and Cu, showing different growth patterns of these two clusters. Charge transfer is found to proceed from M to the Si_n framework in all MSi_n clusters and is stronger for M = Sc than for M = Cu. A mixed ionic and covalent bonding picture between M and Si atoms emerges for MSi_n. Strong hybridization exists between Sc d and Si orbitals in $ScSi_n$, while the d shell of Cu in $CuSi_n$ remains nearly closed and contributes little to the Cu−Si bonding. On the basis of the optimized geometries, various energetic properties are calculated for the most stable isomers of MSi_n, including the binding and fragmentation energies, vertical and adiabatic ionization potentials, and electron affinities. Both the binding and fragmentation energies indicate that MSi_2 and MSi_5 have enhanced stability and could be produced with high abundance in mass spectrum.

1. Introduction

The electronic properties of silicon devices can be profoundly influenced by the presence of doped metal impurities. Extensive experimental and theoretical efforts have been devoted to the behavior of metal impurities in silicon matrix.[1,2] In view of the current miniaturization trend of microelectronic devices, it is expected that the spatial extension of electronic elements will soon approach the size of clusters. In this regime, the structure and properties of materials are size-dependent and are expected to differ dramatically from those of bulk counterparts. Thus, it is of fundamental and technological importance to explore how these well-described and extensively used systems will transform as they are scaled down to cluster dimension. A detailed study on the size dependence of the structures and properties of clusters will greatly deepen our understanding of the formation and bonding mechanisms in metal−silicon composite materials and interfaces. Moreover, the properties characteristic for clusters could be exploited for new technological applications.

Several recent experimental projects have dealt with noble or transition metal (TM)−silicon clusters. In a pioneering mass spectrometric investigation, Beck[3] demonstrated the existence of small mixed metal−silicon clusters in the form of MSi_n with M = Cu, Cr, Mo, and W. Specifically, he observed $CuSi_n$ units in the range of $6 \le n \le 12$ with a pronounced abundance maximum at $n = 10$. This study was complemented more recently by Scherer et al.,[4] who identified experimentally several series of smaller Cu_mSi_n clusters ($m \le 3$, $n \le 9$). The latest experimental achievement related to TM−silicon clusters was reported by Hiura et al.[5] They used an ion trap to detect a cluster series of the form $TMSi_n^+$ (TM = Hf, Ta, W, Re, Ir, etc. with $n = 14, 13, 12, 11, 9$, respectively). According to their interpretation of the experimental findings, the identified clusters contain the metal atoms as endohedral impurities surrounded by polyhedral Si_n cages.

Stimulated by these experimental results, a series of computational investigations has been performed by our group on the geometric and electronic properties of $CuSi_n$ ($n = 4, 6, 8, 10, 12$) using a hybrid density functional technique (B3LYP).[6−8] On the other hand, Han et al. have performed several computational investigations on $TMSi_n$ (TM = Cr, Mo, W) clusters, including $TMSi_{15}$,[9] $CrSi_n$ ($n = 1-6$),[10] $MoSi_n$ ($n = 1-6$),[11] and WSi_n ($n = 1-6, 12$).[12] In addition, there are several recent articles dealing with the systematics of TM-encapsulating cagelike Si_n structures with $n = 14-16$ and TM in several series: Cr, Mo, W; Ti, Zr, Hf; and Fe, Ru, Os.[13,14]

In our previous studies of the geometries, stabilities, and bonding features of low−lying $CuSi_n$ ($n = 4, 6, 8, 10, 12$) isomers,[6−8] the intuitive assumption of the sytem's preference for endohedral impurity sites was critically examined. We found that for $CuSi_n$ with $4 \le n \le 10$, the Si_n frames of the most stable isomers usually adopt the geometries of the ground-state or low-lying isomers of Si_n or Si_{n+1} with Cu occupying various adsorption or substitutional sites and that there is a charge transfer from Cu to the Si_n framework. Similar findings in the geometries and charge transfer have been reported for alkali-metal-doped silicon clusters $NaSi_n$ ($n = 1-7$).[15] Because the Cu atom is characterized by a 4s valence electron and a closed 3d shell, this similarity between $CuSi_n$ and $NaSi_n$ is not unexpected. In contrast, the TM atoms are characterized by open

* To whom correspondence should be addressed. E-mail addresses: xiao@twister.jsums.edu (C.X.); hagx@twister.jsums.edu (F.H.).

10.1021/jp021668y CCC: $22.00
Published on Web 10/19/2002

d shells. In this contribution, we will mainly ask for the influence exerted by the TM atoms on the structures and properties of the Si_n matrixes, the charge transfer between TM and the Si_n framework, the ground-state electronic configuration of $TMSi_n$ clusters, and the distribution of the spin polarization among the cluster constituents. For $TMSi_n$ ($n = 1-6$) clusters with TM = Cr, Mo, and W,[10-12] it has been found that these clusters usually differ from $CuSi_n$ ($n = 4-12$) in their structures and bonding features and the details of the charge-transfer process.[7,8]

In this paper, the impact of Sc and Cu metal atoms on the structures and properties of small Si_n ($n = 1-6$) clusters is studied in a comparative manner. We chose Sc as impurity because it has only one 3d electron and represents the simplest case of the 3d TM series. Another motivation is that a number of Sc-doped fullerenes have been successfully synthesized and extensively studied.[16,17] The paper is laid out as follows: the computational details are described in section 2, the results are presented and discussed in section 3, and our final conclusions are given in section 4.

2. Computational Details

All calculations for MSi_n clusters (M = Sc, Cu; $n = 1-6$) were carried out with the B3LYP hybrid density functional method and the 6-311+G(d) basis set in the Gaussian 98 package.[18] The reliability of the B3LYP/6-311+G(d) approach for the description of Cu-containing Si_n clusters was carefully tested by calculation on the Cu and Si atoms and their dimers.[9] For Sc-containing Si_n systems, we have examined the ground state and ionization potential of the Sc atom, and the calculated results (^{2}D, 6.58 eV) agree well with the experimental ones (^{2}D, 6.56 eV).[19]

Because, according to our findings, the structures of the most stable and low-lying isomers of $CuSi_n$ ($n = 4-10$) correspond to the substitutional structures of Si_{n+1} or the adsorption structures of Si_n and the relaxation of unstable substitutional structures often leads to adsorption geometries,[7,8] in the work presented here, we chose the structures of the ground-state or low-lying isomers of Si_{n+1} as the initial geometries for MSi_n (M = Sc, Cu) with one of the Si atoms replaced by M, and the resulting structures were then fully optimized. Such choice makes it possible to relate the structure of MSi_n to Si_{n+1}. For the smaller MSi_n clusters ($n = 1-4$), the adsorption of M on various surface sites of Si_n in the ground state was also considered to make a comparison with the substitutional structures and make the search for possible low-lying isomers more extensive. The structures for $CuSi_4$ and $CuSi_6$ have already been determined and reported in our previous publications,[6,8] and the structures for other cluster sizes of $CuSi_n$ ($n = 1-3, 5$) were further determined in this study to extend the comparison with $ScSi_n$ to all cluster sizes considered in this work. The harmonic vibrational frequencies were calculated analytically for all stationary points to classify them as local minima or saddle points.

For each initial geometry of MSi_n (M = Sc, Cu, $n = 1-6$), optimizations were performed in both the spin doublet and quartet conditions and several different electronic configurations for a given spin multiplicity were examined with the purpose to determine the most stable one. The doublet states were found to correspond to the ground-state electronic configurations for all MSi_n (M = Sc, Cu) clusters except for the ScSi dimer, which is a spin quartet. Spin contamination is found to be small for all isomers that we have explored.

The structures of pure Si_n clusters in both the neutral and charged forms have been determined by extensive research at the ab initio and density functional levels in previous publications.[20-24] For comparison with the relevant MSi_n clusters, the geometries for the ground-state and low-lying isomers of Si_n, Si_n^+, and Si_n^- ($n = 2-7$) were reoptimized at the B3LYP/6-311+G(d) level.

3. Results and Discussion

In the following, we will first discuss the geometric, electronic, and magnetic properties of individual MSi_n (M = Sc, Cu; $n = 1-6$) species and then examine the size dependences of various energetic properties for the most stable isomers of these series. These properties are summarized in Tables 1-4 and Figures 1-11. The relative energies (also indicated in Figure 1), electronic states, and optimized geometric parameters (bond lengths and angles) for all structures of Si_{n+1} and MSi_n (M = Sc, Cu; $n = 1-6$) clusters at the B3LYP/6-311+G(d) level are available in Supporting Information.

3.1. Individual Clusters. *ScSi and CuSi.* The ground state of Si_2 is known to be a spin triplet ($^3\Sigma_g^-$).[20] The bond length obtained at the B3LYP/6-311+G(d) level is 2.280 Å, which is close to the experimental value of 2.246 Å.[20] This bond length was calculated to be 2.227 and 2.265 Å, respectively, at the HF/6-31G* and MP4/(6s,5p,3d,1f) levels.[20] The highest occupied and lowest unoccupied molecular orbitals (HOMO and LUMO) of Si_2 are both bonding orbitals (see Figure 2). Therefore, removal or addition of an electron in Si_2 will lead to an elongation or a shrinkage of the Si−Si bond length, respectively. Indeed, the bond lengths that we determined for Si_2^+ and Si_2^- are 2.302 and 2.198 Å, respectively, at the B3LYP/6-311+G(d) level. The corresponding data at the HF/6-31G* level are 2.26 and 2.159 Å for Si_2^+ and Si_2^-, respectively.[23,24] The latter result is increased to 2.202 Å at the MP2/6-31G* level,[24] in good agreement with our B3LYP/6-311+G(d) value.

The initial geometries for ScSi and CuSi dimers were obtained by substituting a Si atom in Si_2 dimer with Sc or Cu. By examining several different electronic configurations and relaxing the bond length, we determined the ground state for ScSi and CuSi dimers to be a spin quartet ($^4\Sigma^-$) and doublet ($^2\Pi$), respectively (see Supporting Information). At the B3LYP/6-311+G(d) level, CuSi has a bond length of 2.251 Å, close to the value of 2.280 Å for Si_2, while ScSi adopts a much longer bond length (2.520 Å). The bond lengths obtained for TMSi (TM = Cr, Mo, W) at the B3LYP/LanL2DZ level, in which an effective core potential is used, are close to CuSi, namely, 2.169 Å for CrSi and 2.24 Å for both MoSi and WSi.[10-12] It should be pointed out that care must be taken when comparing with $CrSi_n$,[10] because these clusters were considered under the spin singlet constraint only, while different spin multiplicities were examined for $MoSi_n$ and WSi_n.[11,12]

The binding energies that we obtained at the B3LYP/6-311+G(d) level for ScSi and CuSi are quite close (1.925 and 2.038 eV, respectively), and both values are considerably smaller than that obtained for Si_2 (3.065 eV, see Table 1). Therefore, the Sc−Si and Cu−Si interactions are weaker than the Si−Si interaction.

From Tables 1 and 2, one finds that the binding and fragmentation energies of $ScSi_n$, with respect to isolated atoms and Sc + Si_n, respectively, are usually larger than corresponding values of $CuSi_n$, indicating that the Sc−Si interaction is generally stronger than the Cu−Si interaction, the ScSi and CuSi dimers being the only exception. A final assessment of the relative stability of these dimers, however, should be based on additional calculations employing larger basis set and quantum mechanical procedures of higher level than those used in this work.

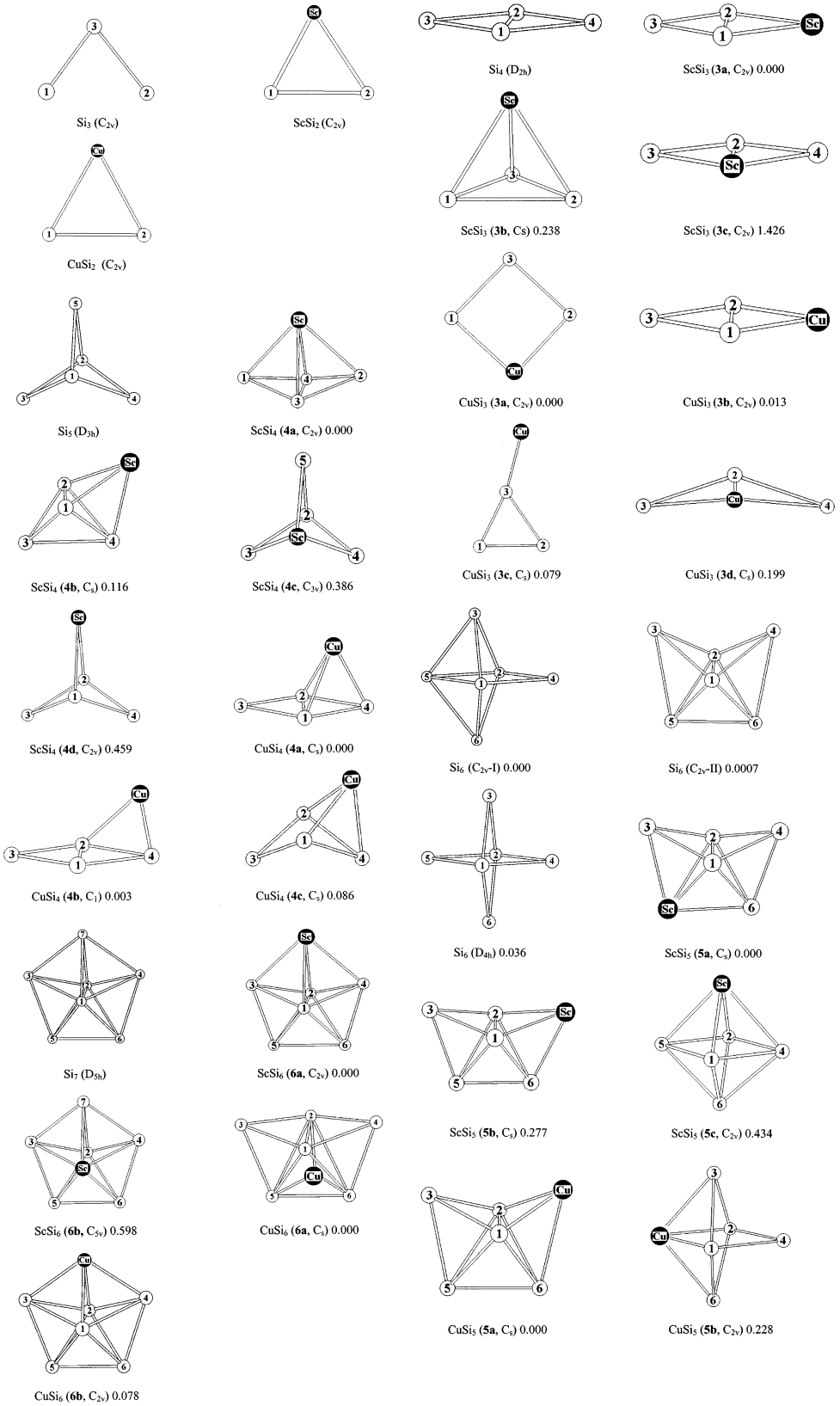

Figure 1. Optimized geometries and relative energies (in eV) of Si_{n+1} and MSi_n (M = Sc, Cu; $n = 1-6$) clusters at the B3LYP/6-311+G(d) level. Open and solid circles stand for Si and M atoms, respectively.

The three unpaired electrons in ScSi occupy the HOMO and the second HOMO (the orbital immediately below the HOMO) of the majority spin (α) and are shared by Sc and Si (see Figure 3). Both of these orbitals are bonding between Sc and Si with dominant Sc s character in the former and considerable Sc d and p characters in the latter. The HOMO of ScSi of the minority spin (β) is also bonding between Sc and Si (see Figure 2), which is composed of dominant Sc s, small Sc d, and significant Si s and p components. For CuSi, the only unpaired electron resides in the α-HOMO, which is essentially localized on the Si atom with dominant Si p and very small Cu d characters (see Figure 3), in contrast to the case of ScSi.

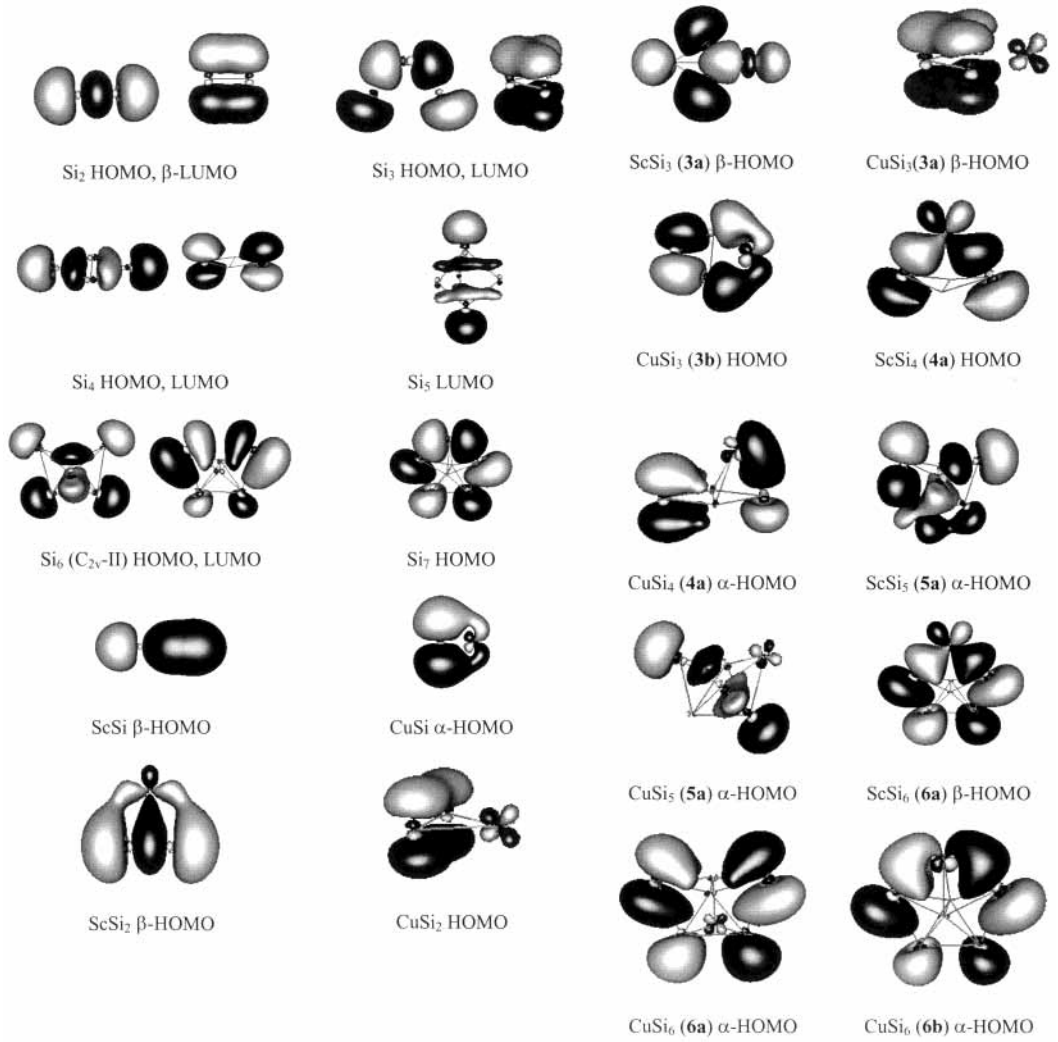

Figure 2. Contour maps of the HOMO of selected MSi_n (M = Sc, Cu) clusters and the HOMO and LUMO of Si_{n+1} ($n = 1-6$) clusters. The lighter and darker lobes correspond to the positive and negative phases of the orbitals, respectively. The orientations of MSi_n clusters are the same as those in Figure 1, except for the LUMO of Si_3, HOMO of $CuSi_2$, and β-HOMO of $CuSi_3$ (**3a**) in which the plane of atoms is shown horizontally and for the LUMO of Si_5 in which the apical axis (1Si−2Si) is shown vertically.

TABLE 1: Binding Energies Per Atom (E_b, in eV) of the Most Stable Isomers of MSi_n (M = Sc, Cu; $n = 1-6$) and Si_{n+1} ($n = 1-7$) at the B3LYP/6-311+G(d) Level

cluster	E_b	cluster	E_b	cluster	E_b
ScSi	0.963	CuSi	1.019	Si_2	1.533
$ScSi_2$	1.992	$CuSi_2$	1.885	Si_3	2.235
$ScSi_3$	2.402	$CuSi_3$	2.180	Si_4	2.719
$ScSi_4$	2.653	$CuSi_4$	2.466	Si_5	2.837
$ScSi_5$	2.899	$CuSi_5$	2.722	Si_6	3.000
$ScSi_6$	2.948	$CuSi_6$	2.805	Si_7	3.100
				Si_8	3.024

$ScSi_2$ and $CuSi_2$. The ground state of Si_3 is an isosceles triangle with C_{2v} symmetry (see Figure 1) in a singlet state ($^1A_1$).[20] The HOMO is bonding between the top (3Si) and two bottom (1Si and 2Si) atoms but antibonding between the two bottom atoms, while the LUMO is bonding among all atoms (see Figure 2). As a result, Si_3 has two short lateral bond lengths (1Si−3Si, 2Si−3Si) of 2.185 Å and a long bottom bond length (1Si−2Si) of 2.877 Å or a large top bond angle (1Si−3Si−2Si) of 82.348° at the B3LYP/6-311+G(d) level. Either the removal or addition of an electron in Si_3 will lead to a reduction in the bottom bond length and accordingly in the top bond angle, which adopt the values of 2.153 Å and 52.677° for Si_3^+ and 2.453 Å and 65.624° for Si_3^- at the B3LYP/6-311+G(d) level.

TABLE 2: Fragmentation Energy (E_f, in eV) of the Most Stable Isomers of MSi_n (M = Sc, Cu; $n = 1-6$) with Respect to Sc + Si_n or Si + $ScSi_{n-1}$ and for Si_{n+1} with Respect to Si + Si_n at the B3LYP/6-311+G(d) Level

fragmentation process	E_f	fragmentation process	E_f
ScSi → Sc + Si	1.925	CuSi → Cu + Si	2.038
$ScSi_2$ → Sc + Si_2	2.912	$CuSi_2$ → Cu + Si_2	2.589
$ScSi_2$ → Si + ScSi	4.051	$CuSi_2$ → Si + CuSi	3.616
$ScSi_3$ → Sc + Si_3	2.903	$CuSi_3$ → Cu + Si_3	2.017
$ScSi_3$ → Si + $ScSi_2$	3.631	$CuSi_3$ → Si + $CuSi_2$	3.067
$ScSi_4$ → Sc + Si_4	2.389	$CuSi_4$ → Cu + Si_4	1.453
$ScSi_4$ → Si + $ScSi_3$	3.659	$CuSi_4$ → Si + $CuSi_3$	3.609
$ScSi_5$ → Sc + Si_5	3.210	$CuSi_5$ → Cu + Si_5	2.148
$ScSi_5$ → Si + $ScSi_4$	4.129	$CuSi_5$ → Si + $CuSi_4$	4.003
$ScSi_6$ → Sc + Si_6	2.639	$CuSi_6$ → Cu + Si_6	1.636
$ScSi_6$ → Si + $ScSi_5$	3.241	$CuSi_6$ → Si + $CuSi_5$	3.300
Si_2 → Si + Si	3.065	Si_3 → Si + Si_2	3.639
Si_4 → Si + Si_3	4.173	Si_5 → Si + Si_4	3.308
Si_6 → Si + Si_5	3.812	Si_7 → Si + Si_6	3.703
Si_8 → Si + Si_7	2.490		

The initial geometries for MSi_2 (M = Sc, Cu) were constructed by substituting M for any Si atom of Si_3 (C_{2v}) or by adsorbing M over the midpoint of Si_2. Relaxation of all of these structures leads to the same isosceles triangular structure for MSi_2 (see Figure 1).

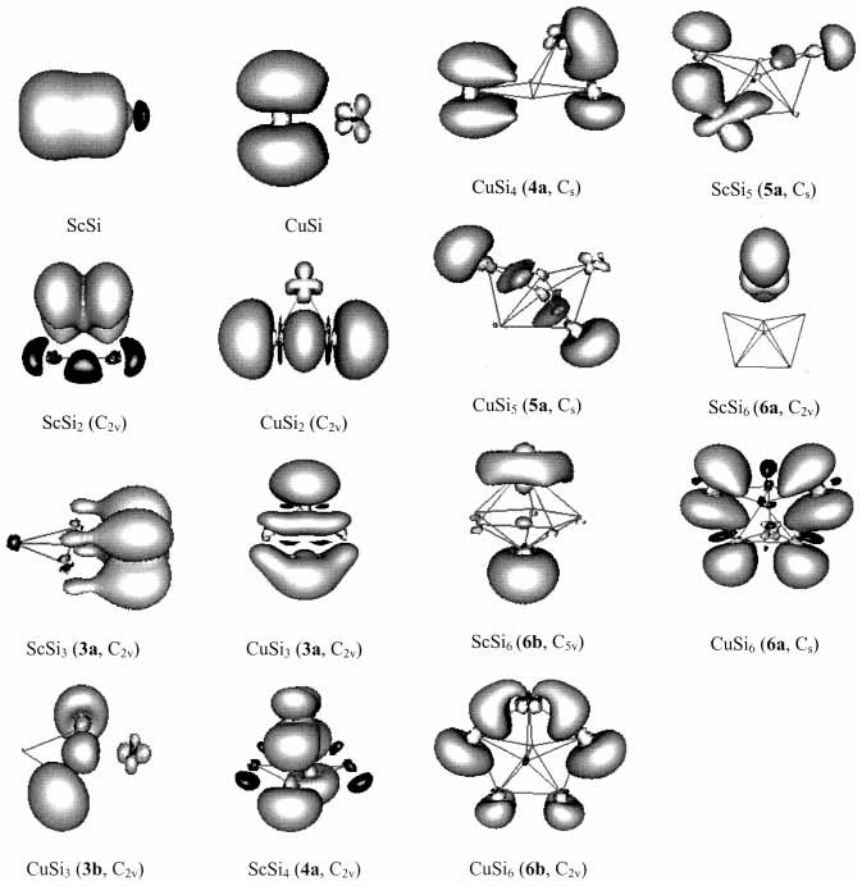

Figure 3. Contour maps of the spin density of selected MSi_n (M = Sc, Cu; $n = 1-6$) clusters. The lighter and darker lobes correspond to the up and down spin polarizations, respectively. The orientations of MSi_n clusters are the same as those in Figure 1, except for $ScSi_6$ (**6b**), in which the apical axis (Sc−2Si) is shown vertically with Sc at the top.

The M−Si bond lengths in MSi_2 (M = Sc, Cu) are 2.576 and 2.337 Å for M = Sc and Cu, respectively, at the B3LYP/6-311+G(d) level, which are close to corresponding values in MSi dimers. The bottom bond length (1Si−2Si) and accordingly the top bond angle (1Si−M−2Si) in MSi_2 are much reduced as compared with Si_3, which adopt the values of 2.877 Å and 82.348° in Si_3, 2.177 Å and 50.006° in $ScSi_2$, and 2.170 Å and 55.320° in $CuSi_2$. Note that the bond length for Si_2 and Si_2^+ are similar (2.280 and 2.302 Å, respectively), while the bond length for Si_2^- is shorter (2.198 Å). Therefore, the Si−Si bond length in MSi_2 is close to the Si−Si bond length in Si_2^-, suggesting that MSi_2 may be understood as an adsorption structure of Si_2 with a charge transfer from M to Si_2. From Table 3, one finds that the Sc and Cu atoms have a positive natural charge of 0.69*e* and 0.40*e*, respectively, in $ScSi_2$ and $CuSi_2$ in keeping with the conclusion based on the geometric structures. This charge-transfer picture is consistent with the findings in larger $CuSi_n$ ($n = 4-12$) and $NaSi_n$ ($n = 2-6$) clusters,[8,15] where the charge is transferred from Cu or Na to the Si_n framework but is in contrast to the observations in $TMSi_n$ (TM = Cr, Mo, W) clusters,[10−12] where the charge transfer is found to proceed in the opposite direction, that is, from Si_n to TM. The result that a stronger charge transfer occurs from Sc to Si_2 in $ScSi_2$ than that from Cu to Si_2 in $CuSi_2$ is consistent with the smaller electronegativity of Sc (1.3) as compared to Cu (1.9).

The structures obtained for $TMSi_2$ (TM = Cr, Mo, W) are also isosceles triangles.[10−12] At the B3LYP/LanL2DZ level, the calculated TM−Si bond lengths are nearly the same for all three TM atoms, being 2.21, 2.25, and 2.28 Å for TM = Cr, Mo, and W, respectively, which are close to the Cu−Si bond length in $CuSi_2$. However, the bottom bond lengths and the top bond angles in these configurations are considerably larger than those found in MSi_2 (M = Sc, Cu).

Although $ScSi_2$ and $CuSi_2$ have similar structures, their electronic and spin polarization features are different (see Figures 2 and 3). The β-HOMO and the second α-HOMO of $ScSi_2$ both correspond to the HOMO of Si_2 and are bonding among the atoms with significant Sc d and large Si s and p characters. The unpaired electron of $ScSi_2$ resides in the α-HOMO, which is localized on the Sc atom with nearly pure Sc d character, in contrast to the case of ScSi. The HOMO and second α-HOMO for $CuSi_2$ correspond to the β-LUMO and HOMO of Si_2, respectively, both of which are bonding between the Si atoms and are only slightly influenced by Cu. As a result, the unpaired electron of $CuSi_2$, which occupies the second α-HOMO, is essentially situated on the two Si atoms with little contribution from Cu, similar to the observation made on CuSi.

$ScSi_3$ and $CuSi_3$. The ground state of Si_4 is a planar rhombus with D_{2h} symmetry (see Figure 2) in a singlet state (^1A_g).[20] Its HOMO is bonding among all atoms with large p components on atoms of the short diagonal (1Si, 2Si) and large s and p components on atoms of the long diagonal (3Si, 4Si), while its LUMO is composed of the p orbitals on atoms of the long diagonal and is weakly antibonding between them (see Figure 2). The geometry of Si_4^- (D_{2h}) is very close to that of neutral Si_4, with only slight relaxation.[24]

By substituting M (M = Sc, Cu) for Si atoms of Si_4 (D_{2h}) or by capping M on various adsorption sites of Si_3 (C_{2v}) and relaxing the resulting geometries, we have identified three isomers for $ScSi_3$ and four isomers for $CuSi_3$ (see Figure 1).

TABLE 3: Natural Charges and Natural Spin Populations for Atoms in MSi_n and Si_{n+1} (M = Sc or Cu; n = 1−6) Clusters

			M	Si(1)	Si(2)	Si(3)	Si(4)	Si(5)	Si(6)	Si(7)
ScSi	$C_{\infty v}$	charge	0.41	−0.41						
		spin	1.36	1.64						
CuSi	$C_{\infty v}$	charge	0.03	−0.03						
		spin	−0.02	1.02						
Si_2	$D_{\infty h}$	charge	0.00	0.00						
$ScSi_2$	C_{2v}	charge	0.69	−0.35	−0.35					
		spin	1.09	−0.04	−0.04					
$CuSi_2$	C_{2v}	charge	0.40	−0.20	−0.20					
		spin	0.02	0.49	0.49					
Si_3	C_{2v}	charge		0.20	0.20	−0.41				
$ScSi_3$	**3a**	charge	0.87	−0.47	−0.47	0.08				
		spin	0.99	0.04	0.04	−0.08				
	3b	charge	0.65	−0.24	−0.24	−0.18				
		spin	0.52	0.30	0.30	−0.12				
	3c	charge	0.47		−0.27	−0.10	−0.10			
		spin	0.54		0.44	0.01	0.01			
$CuSi_3$	**3a**	charge	0.40	−0.11	−0.11	−0.18				
		spin	0.25	0.05	0.05	0.66				
	3b	charge	0.51	−0.21	−0.21	−0.08				
		spin	0.06	0.49	0.49	−0.04				
	3c	charge	0.43	−0.01	0.04	−0.46				
		spin	0.00	0.37	0.35	0.29				
	3d	charge	0.53		−0.48	−0.02	−0.02			
		spin	0.04		−0.12	0.54	0.54			
Si_4	D_{2h}	charge		−0.23	−0.23	0.23	0.23			
$ScSi_4$	**4a**	charge	0.95	−0.11	−0.11	−0.36	−0.36			
		spin	0.47	0.37	0.37	−0.11	−0.11			
	4b	charge	0.78	−0.28	−0.28	0.02	−0.25			
		spin	0.38	0.12	0.12	0.00	0.37			
	4c	charge	0.75		−0.01	−0.25	−0.25	−0.25		
		spin	0.16		0.40	0.15	0.15	0.15		
	4d	charge	0.88	−0.55	−0.55	0.12	0.12			
		spin	1.05	−0.01	−0.01	−0.01	−0.01			
$CuSi_4$	**4a**	charge	0.47	−0.19	−0.19	0.04	−0.12			
		spin	0.11	0.01	0.01	0.53	0.33			
	4b	charge	0.48	−0.06	−0.36	0.10	−0.16			
		spin	0.15	0.04	−0.02	0.46	0.37			
	4c	charge	0.50	−0.03	−0.12	−0.18	−0.18			
		spin	0.05	0.50	0.29	0.08	0.08			
Si_5	D_{3h}	charge		−0.22	−0.22	0.15	0.15	0.15		
$ScSi_5$	**5a**	charge	0.84	−0.30	−0.30	−0.10	0.10		−0.24	
		spin	0.42	0.00	0.00	0.38	0.18		0.02	
	5b	charge	0.95	−0.40	−0.40	0.07		0.01	−0.24	
		spin	0.75	−0.02	−0.02	0.09		0.10	0.10	
	5c	charge	0.33	−0.32	−0.32		−0.08	−0.08	−0.04	
		spin	0.27	0.40	0.40		−0.03	−0.03	−0.01	
$CuSi_5$	**5a**	charge	0.52	−0.22	−0.22	0.03		−0.09	−0.03	
		spin	0.01	0.04	0.04	0.49		−0.01	0.43	
	5b	charge	0.55	−0.22	−0.22	−0.04	−0.05		−0.04	
		spin	0.04	0.04	0.04	0.44	0.03		0.44	
Si_6	C_{2v}-I	charge		−0.30	−0.30	0.13	0.27	0.06	0.13	
	C_{2v}-II	charge		−0.29	−0.29	0.22	0.22	0.07	0.07	
	D_{4h}	charge		−0.28	−0.28	0.14	0.14	0.14	0.14	
$ScSi_6$	**6a**	charge	0.80	−0.31	−0.31	−0.21	−0.21	0.12	0.12	
		spin	0.99	0.02	0.02	−0.01	−0.01	0.00	0.00	
	6b	charge	1.06		−0.19	−0.17	−0.17	−0.17	−0.17	−0.17
		spin	0.29		0.54	0.03	0.03	0.03	0.03	0.03
$CuSi_6$	**6a**	charge	0.52	−0.25	−0.31	0.12	0.12	−0.10	−0.10	
		spin	0.00	0.00	−0.04	0.28	0.28	0.24	0.24	
	6b	charge	0.63	−0.32	−0.32	−0.03	−0.03	0.03	0.03	
		spin	0.03	−0.01	−0.01	0.38	0.38	0.12	0.12	
Si_7	D_{5h}	charge		−0.27	−0.27	0.11	0.11	0.11	0.11	0.11

All of these isomers are confirmed to be local minima on the respective potential energy surfaces by vibrational analysis.

The substitution of Sc or Cu for Si atoms of the long diagonal (3Si, 4Si) in Si_4 (D_{2h}) rhombus results in $ScSi_3$ (**3a**) and $CuSi_3$ (**3b**), respectively (see Figure 1). In both cases, the rhombic framework of Si_4 is maintained with Si−Si bond lengths relaxed only by 1−2%, and the M−Si (M = Sc, Cu) bond length is similar to those found in MSi and MSi_2. Therefore, $ScSi_3$ (**3a**) and $CuSi_3$ (**3b**) represent two typical substitutional structures; they are the most stable and the second most stable structures that we have identified for these two clusters, respectively.

As in the case of MSi_2 (M = Sc, Cu), the Si_3 framework in $ScSi_3$ (**3a**) and $CuSi_3$ (**3b**) can be much more naturally related to anionic Si_3^- (C_{2v}) than to neutral Si_3 (C_{2v}). This can be seen by comparing the 1Si−2Si bond length and the 1Si−3Si−2Si bond angle for $ScSi_3$ (**3a**, 2.453 Å and 64.387°) and $CuSi_3$ (**3b**,

2.435 Å and 64.254°) with the corresponding values for Si_3 (2.877 Å and 82.348°) and Si_3^- (2.453 Å and 65.624°). Therefore, $ScSi_3$ (**3a**) and $CuSi_3$ (**3b**) can also be described as adsorption structures, characterized by substantial electron transfer from Sc or Cu to the Si_3 framework.

From Table 3, one finds that the Sc and Cu atoms in $ScSi_3$ (**3a**) and $CuSi_3$ (**3b**) have a positive charge of 0.87*e* and 0.51*e*, respectively. Therefore, the Sc atom in $ScSi_3$ (**3a**) and Cu atom in $CuSi_3$ (**3b**) are in a charge state (i.e., positive) similar to that of the substituted Si atoms of the long diagonal ($q = 0.23e$) in Si_4 (D_{2h}). The substitution of Sc or Cu for these Si atoms of Si_4 (D_{2h}) will not introduce any major charge rearrangement in the cluster. This may account for the stability of this substitutional structure. In contrast, atoms of the short diagonal in Si_4 (D_{2h}) have a negative charge ($q = -0.23e$) and the substitution of Sc or Cu for these atoms is expected to induce a larger charge redistribution and larger structural reconstruction.

Indeed, the substitution of Sc for atoms of the short diagonal in Si_4 (D_{2h}) rhombus is unstable, and the structure is relaxed to $ScSi_3$ (**3a**). It is interesting that, by inspecting more electronic configurations, we could identify another doublet isomer $ScSi_3$ (**3c**) in which Sc is located at the substitutional site of the short diagonal, but it is less stable than $ScSi_3$ (**3a**) by 1.426 eV. This finding documents the importance of examining different electronic configurations for a given initial structure and given spin multiplicity to determine the most stable one. We found that this is very important, as well as challenging, for both $ScSi_n$ and $CuSi_n$. To be concise, we only report the most stable structure for isomers of similar geometric configurations in this paper.

The substitution of Cu for atoms of the short diagonal in Si_4 (D_{2h}) leads to a butterfly-like structure $CuSi_3$ (**3d**), which is a bent rhombus with a downward opening angle of 153.759° and is higher than $CuSi_3$ (**3b**) by 0.199 eV.

In addition to substitutional structures, we have also considered adsorption of Sc or Cu on various sites of the Si_3 (C_{2v}) framework. The Sc or Cu atom was capped to the 1Si−2Si bridge to form a planar rhombus, adsorbed to the center of Si_3 triangle to form a tetrahedral structure, or adsorbed above the top atom (3Si) to form an upside-down Y-shaped structure, and these initial geometries were fully optimized.

The adsorption of Sc on the bottom bridge (1Si−2Si) of Si_3 (C_{2v}) reproduces the substitutional structure $ScSi_3$ (**3a**), while adsorption of Cu on the same site of Si_3 (C_{2v}) will yield a squarelike structure $CuSi_3$ (**3a**), which is lower than the rhombic substitutional structure $CuSi_3$ (**3b**) only by 0.013 eV. The squarelike structure is a transition state for $ScSi_3$, and it collapses to rhombic $ScSi_3$ (**3a**) with an energy gain of 1.450 eV.

The adsorption of Sc to the center of Si_3 (C_{2v}) triangle results in a stable tetrahedral structure $ScSi_3$ (**3b**), which is higher than $ScSi_3$ (**3a**) by 0.238 eV. In contrast, the adsorption of Cu at the same site is unstable, and the relaxation reproduces the butterfly-like structure $CuSi_3$ (**3d**).

The last adsorption structure that we have considered is the adsorption of Sc or Cu over the top atom (3Si) of Si_3 (C_{2v}) to form an upside-down Y-shaped structure. For $ScSi_3$, this top-adsorbed structure is unstable and transforms into the most stable rhombic structure $ScSi_3$ (**3a**). For $CuSi_3$, the symmetric top adsorption corresponds to a second-order saddle point and relaxation leads to isomer $CuSi_3$ (**3c**), which lies only 0.079 eV higher than the most stable isomer $CuSi_3$ (**3a**).

In two previous contributions, the substitutional effect of TM (TM = Cr, Mo) on Si_4 (D_{2h}) rhombus was examined.[10,11] In contrast to the results of MSi_3 (M = Sc, Cu), in which the M atom prefers the substitutional sites of the long diagonal in Si_4 (D_{2h}), the TM atoms were found to substitute preferentially for atoms of the short diagonal. This demonstrates the correlation between the charge state and the substitutional behavior of metal atoms in MSi_n (M = Sc, Cu) and $TMSi_n$ (TM = Cr, Mo, W) clusters.

The bonding nature and spin distributions in MSi_3 (M = Sc, Cu) clusters can be analyzed by examining their frontier molecular orbitals and by natural spin population analysis (see Figures 2 and 3 and Table 3). For $ScSi_3$ (**3a**), the β-HOMO and second α-HOMO both have significant s and p characters on all Si atoms, and large s and considerable d characters on the Sc atom, leading to a bonding interaction between Sc and the atoms of the short diagonal (1Si, 2Si) but antibonding interaction between 3Si and the latter (see Figure 2). The unpaired electron of $ScSi_3$ (**3a**) resides in the α-HOMO, which is localized on the Sc atom with dominant Sc d character (see Figure 3), similar to the case of $ScSi_2$.

Although $CuSi_3$ (**3a)** and $CuSi_3$ (**3b)** are nearly isoenergetic and both adopt the doublet state of $^2A_1$, they differ with respect to the geometric, electronic, and magnetic structures. For the squarelike $CuSi_3$ (**3a**), the β-HOMO and the second α-HOMO both correspond to the LUMO of Si_3, which contains large p components on all Si atoms and is bonding among them with only small admixture of Cu p and d characters (see Figure 2). The unpaired electron in $CuSi_3$ (**3a**) occupies the α-HOMO, which is bonding among all atoms of the cluster (see Figure 3).

For rhombic $CuSi_3$ (**3b**), the HOMO of both spins corresponds to the HOMO of Si_3 with noticeable Cu p and d characters mixed in, leading to a bonding interaction among the Si atoms and also between Cu and the Si_3 framework (see Figure 2). The unpaired electron in $CuSi_3$ (**3b**) resides in the second α-HOMO, which is essentially shared by the two Si atoms of the short diagonal with little contribution from Cu. This spin distribution is similar to the observations made on CuSi and $CuSi_2$ but is in contrast to the case of $CuSi_3$ (**3a**) (see Figure 3).

The charge and spin distributions for all MSi_3 (M = Sc, Cu) isomers are recorded in Table 3. In all species, the charge transfer is found to proceed from M to the neighboring Si atoms. The unpaired electrons in both $ScSi_3$ (**3b**) and $ScSi_3$ (**3c**) are delocalized over Sc and the Si atoms, in contrast to the findings in $ScSi_2$ and $ScSi_3$ (**3a**). For $CuSi_3$ (**3c**) and $CuSi_3$ (**3d**), the spin is spread over the Si atoms with little contribution from Cu. This is different from the case of $CuSi_3$ (**3a**) but similar to the observations made on CuSi, $CuSi_2$, and $CuSi_3$ (**3b**).

$ScSi_4$ and $CuSi_4$. The ground state of Si_5 is a compressed trigonal bipyramid with D_{3h} symmetry (see Figure 1) in a singlet state ($1A_1'$),[20] which can be described as a downward bent rhombus (1Si through 4Si) capped with a Si atom (5Si) over the 1Si−2Si bridge.

The LUMO of Si_5 (D_{3h}) is bonding among the equatorial atoms (3Si through 5Si) and between the apical (1Si, 2Si) and the equatorial atoms, but antibonding between the apical atoms (see Figure 2). As a result, when going from Si_5 (D_{3h}) to Si_5^- (D_{3h}), the distance between the equatorial atoms (3Si−4Si) is reduced by 13.6% (from 3.124 to 2.778 Å) while the distance between the apical atoms (1Si−2Si) is elongated by 17.1% (from 2.947 to 3.451 Å). Therefore, the short (1Si−2Si) and long (3Si−4Si) diagonals of the bent rhombus are interchanged as one goes from Si_5 (D_{3h}) to Si_5^- (D_{3h}).

The initial structures of MSi_4 (M = Sc, Cu) were built by substitution of M for Si atoms in Si_5 (D_{3h}) or by adsorption of M over the center of Si_4 (D_{2h}) rhombus, and the resulting

geometries were fully optimized. Because the equatorial atoms of Si_5 (D_{3h}) have a positive charge while that of the apical atoms is negative (see Table 3), it can be expected that the equatorial substitution will be preferred over the apical substitution. Four stable isomers were identified for $ScSi_4$ and three for $CuSi_4$ (see Figure 1). The structures of $CuSi_4$ were reported in our previous papers.[6,8]

The substitution of Sc or Cu for the equatorial atoms of Si_5 (D_{3h}) leads to three isomers for $ScSi_4$ (**4a**, **4b**, **4d**) and one isomer for $CuSi_4$ (**4c**). The short (1Si−2Si) and long (3Si−4Si) diagonals of the bent rhombus in Si_5 (D_{3h}) are interchanged in $ScSi_4$ (**4a**) and $CuSi_4$ (**4c**). Obviously, this behavior constitutes a parallel between MSi_4 (M = Sc, Cu) and Si_5^- (D_{3h}). $ScSi_4$ (**4a**) can be described as the adsorption of Sc over a bent rhombus with an opening angle of 154.379°. For $CuSi_4$ (**4c**), the symmetric top adsorption of Cu over the 1Si−2Si bridge defines a transition state. Upon relaxation of this structure, Cu moves closer to 4Si, albeit with a very small energy gain of 0.037 eV. Despite the apparent structural similarity of $ScSi_4$ (**4b**) and $CuSi_4$ (**4c**), they are substantially different in the 1Si−2Si bond length (2.744 vs 3.446 Å). $ScSi_4$ (**4d**) represents a stable substitutional structure of Si_5 (D_{3h}) with relaxation in the 1Si−2Si and 1Si−3Si bond lengths, as well as in the opening angle of the bent rhombus (1Si−4Si) by 5.1%, 0.3%, and 3.1%, respectively. $ScSi_4$ (**4a**) is lower in energy than $ScSi_4$ (**4b**) and $ScSi_4$ (**4d**) by 0.116 and 0.386 eV, respectively, and is the most stable isomer that we have identified for this cluster.

The substitution of Sc for the apical atoms of Si_5 (D_{3h}) results in a stable substitutional structure $ScSi_4$ (**4c**). As expected from charge analysis, this isomer is less stable than $ScSi_4$ (**4a**), which is derived from equatorial substitution. The replacement of the apical atoms with Cu leads to dramatic reconstruction, and the final structure $CuSi_4$ (**4b**) turns out to be an adsorption geometry in which the Cu atom is capped to an edge (2Si−4Si) of a nearly planar Si_4 rhombus (upward opening angle = 180.839°), adopting an out-of-plane position.

The adsorption of Sc over the center of Si_4 (D_{2h}) rhombus reproduces the substitutional configuration $ScSi_4$ (**4d**), while such adsorption of Cu leads to isomer $CuSi_4$ (**4a**), in which the rhombus is nearly maintained (upward opening angle = 179.608°) and the Cu atom relaxes to an asymmetric position along the long diagonal. $CuSi_4$ (**4a**) is nearly isoenergetic with $CuSi_4$ (**4b**) and $CuSi_4$ (**4c**) with minute energy separations of 0.003 and 0.086 eV, respectively.

The HOMO of $ScSi_4$ (**4a**) and the α-HOMO of $CuSi_4$ (**4a**) both correspond to the LUMO of Si_4 (D_{2h}). They have significant d and p characters on the Sc atom or s and p characters on the Cu atom, combined with large p components on the two Si atoms of the long diagonal of the rhombus. This reflects a bonding interaction between Sc or Cu and the Si atoms of the long diagonal (see Figure 2).

The unpaired electron in $ScSi_4$ (**4a**) and $CuSi_4$ (**4a**) resides in their second α-HOMO and α-HOMO, respectively. The unpaired electron in $ScSi_4$ (**4a**) is shared by Sc and the two Si atoms of the short diagonal (see Figure 3 and Table 3). This spin-polarization feature is similar to ScSi dimer but in contrast to the findings in $ScSi_2$ (**2a**) and $ScSi_3$ (**3a**) in which the unpaired electron is localized on the Sc atom. For $CuSi_4$ (**4a**), the unpaired electron is shared predominantly by the two Si atoms of the long diagonal, but also Cu contributes noticeably to it (see Figure 3 and Table 3). This is similar to the finding in $CuSi_3$ (**3a**) but different from the cases of CuSi dimer, $CuSi_2$, and $CuSi_3$ (**3b**).

The natural charges and natural spin populations for all MSi_4 isomers are listed in Table 3. Just as in smaller MSi_n clusters, electric charge migrates from M to the neighboring Si atoms of Si_4 framework in all MSi_4 clusters. The spin polarization has a minor contribution from the metal atoms in $ScSi_4$ (**4c**) and in all $CuSi_4$ isomers; it is shared by Sc with the neighboring atoms (1Si, 2Si, 4Si) in $ScSi_4$ (**4b**), and localized on the Sc atom in $ScSi_4$ (**4d**).

$ScSi_5$ and $CuSi_5$. Si_6 has three low-lying isomers that are very close in energy (see Figure 1): an edge- and a face-capped trigonal bipyramid (C_{2v}-I and C_{2v}-II) and a compressed octahedron (D_{4h}).[20] At the B3LYP/6-311+G(d) level, the C_{2v}-I isomer is the ground state while the C_{2v}-II and D_{4h} isomers are both transition states that are higher than the C_{2v}-I isomer only by 0.0007 and 0.035 eV, respectively. The ground state of Si_6^- adopts the C_{2v}-II structure.[22] This structure can also be regarded as a bent rhombus (1Si−4Si) capped with a 5Si−6Si dimer.

The LUMO of Si_6 (C_{2v}-II) has large s and p characters on the two top atoms (3Si, 4Si) and is antibonding between them (see Figure 2). As a result, when an extra electron is added to Si_6 (C_{2v}-II) to form Si_6^- (C_{2v}-II), the bent rhombus (1Si through 4Si) is dramatically flattened with the opening angle enlarged by 31.9% (from 115.032 in Si_6 to 151.773° in Si_6^-), while the 3Si−5Si−6Si angle is increased by 9.9% (from 99.132° to 108.957°).

The possible initial structures of MSi_5 (M = Sc, Cu) were constructed from substitution of M for Si atoms of Si_6 (C_{2v}-I, C_{2v}-II, D_{4h}), and the resulting structures were fully optimized. Because the apical atoms (1Si and 2Si) of the three Si_6 isomers have negative charges while the equatorial atoms (3Si through 6Si) have positive charges, one can expect that the substitution of M for the equatorial atoms will be more favorable than the substitution for the apical atoms. Conversely, a preference for apical substitution can be expected for Cr, Mo, and W. In addition, considering that the three isomers of Si_6 are topologically related and nearly isoenergetic, one can also expect that many different substitutions would result in identical structures. Indeed, only three isomers for $ScSi_5$ and two for $CuSi_5$ were identified (see Figure 1).

The most stable isomers of $ScSi_5$ (**5a**) and $CuSi_5$ (**5a**) correspond to Si_6 (C_{2v}-II) with Sc and Cu at the 5Si and 4Si substitutional sites, respectively. The different substitutional sites of Sc in $ScSi_5$ (**5a**) and Cu in $CuSi_5$ (**5a**) can be understood by referring to the different structures of $ScSi_4$ (**4a**) and $CuSi_4$ (**4a**). As seen in Figure 1, $ScSi_5$ (**5a**) and $CuSi_5$ (**5a**) can be visualized to emerge, respectively, from $ScSi_4$ (**4a**) and $CuSi_4$ (**4a**) by capping an additional Si atom to the bottom of the 1Si−4Si rhombus. Because the trigonal bipyramidal framework of Si_5 (D_{3h}) is maintained in $CuSi_5$ (**5a**), it can also be regarded as an adsorption structure. This is supported by the striking similarity between the α-HOMO of $CuSi_5$ (**5a**) and the LUMO of Si_5 (D_{3h}) (see Figure 2).

The second substitutional isomer that we identified for $ScSi_5$ (**5b**) has a structure similar to $CuSi_5$ (**5a**). It is higher than $ScSi_5$ (**5a**) by 0.277 eV. Interestingly, both $ScSi_5$ (**5a**) and $ScSi_5$ (**5b**) can be generated from $ScSi_4$ (**4b**) by capping the 1Si−2Si−Sc or 1Si−2Si−3Si face of $ScSi_4$ (**4b**), respectively, with the additional Si atom.

The last isomer that we obtained for $ScSi_5$ (**5c**) and $CuSi_5$ (**5b**) is a substitutional structure based on Si_6 (D_{4h}) or Si_6 (C_{2v}-I). These units are higher than the most stable isomers $ScSi_5$ (**5a**) or $CuSi_5$ (**5a**) by 0.434 or 0.228 eV, respectively. The square of the equatorial atoms (3Si through 6Si) in Si_6 (D_{4h}) is largely maintained in $ScSi_5$ (**5c**) with Sc occupying the top equatorial site (3Si), while the 1Si−2Si bond length (3.238 Å)

is elongated by as much as 18.3%. Thus, the structure approaches octahedral symmetry.

For WSi_5,[12] a structure similar to $ScSi_5$ (**5c**) is obtained, but the 1Si−2Si−4Si−5Si rhombus turns out to be a nearly perfect planar square with W and the remaining Si atom capped above or below the center of this square, respectively. In addition, the Si atoms of this square all adopt a positive charge (0.15*e* each), while the capped W and Si atoms have a negative charge (−0.52*e* and −0.08*e*). Therefore, the W atom in WSi_5 should be understood as occupying the apex substitutional site of Si_6 (D_{4h}), as expected on the basis of charge analysis. A similar result was reported for $MoSi_5$.[11]

The bonding mechanism operative in $ScSi_5$ (**5a**) and $CuSi_5$ (**5a**) can be understood by relating their electronic structures to Si_6 (C_{2v}-II) or Si_5 (D_{3h}), respectively. As seen in Figure 2, the α-HOMO of $ScSi_5$ (**5a**) corresponds to the HOMO of Si_6 (C_{2v}-II), in which the large s and p characters of 5Si in Si_6 (C_{2v}-II) are replaced by the large d and p characters of Sc in $ScSi_5$ (**5a**). The Sc atom forms strong bonds with neighboring Si atoms in this orbital. On the other hand, the α-HOMO of $CuSi_5$ (**5a**) corresponds to the LUMO of Si_5 (D_{3h}) with little contribution from Cu. The unpaired electron of $ScSi_5$ (**5a**) and $CuSi_5$ (**5a**) is situated in the α-HOMOs of these units (see Figure 3 and Table 3).

The charge and spin distributions of all investigated MSi_5 (M = Sc, Cu) clusters are listed in Table 3. As expected, the M atom behaves as an electron donor in all cases. The unpaired electron is mainly situated on the Sc atom in $ScSi_5$ (**5b**) with a small part spreading over the 3Si, 5Si, and 6Si atoms, while it is shared by Sc, 1Si, and 2Si atoms in $ScSi_5$ (**5c**). The spin distribution in $CuSi_5$ (**5b**) is similar to that in $CuSi_5$ (**5a**), in both of which the unpaired electron is essentially shared by the 3Si and 6Si atoms of the Si_5 framework.

$ScSi_6$ and $CuSi_6$. The ground state of neutral Si_7 is a pentagonal bipyramid with D_{5h} symmetry (see Figure 1) in a singlet state ($^1A_1'$),[21] which can be described as the adsorption of 7Si over the 3Si−4Si bridge of Si_6 (C_{2v}-II) framework. The HOMO of Si_7 (D_{5h}) corresponds to the LUMO of Si_6 (C_{2v}-II), which has little components on the apical atoms (1Si, 2Si) but large p component on 7Si and large s and p components on all other equatorial atoms (3Si through 6Si), leading to strong bonds between 7Si and the two neighboring equatorial atoms (3Si, 4Si) (see Figure 2).

By substituting M (M = Sc or Cu) for the apical or equatorial atoms in Si_7 (D_{5h}) and relaxing the substitutional structures thus generated, we identified two isomers for MSi_6 (see Figure 1). Because the apical and equatorial atoms of Si_7 (D_{5h}) have negative and positive charges, respectively (see Table 3), one can expect that the equatorial substitution will be preferred over the apical substitution for M = Sc and Cu and that the order of preferences will be reversed for M = Cr, Mo, and W. In addition, we have examined the possible existence of stable endohedral structures by positioning M at the center of a compressed or regular octahedron of Si_6 (D_{4h} or O_h).

For $ScSi_6$, the framework of Si_7 (D_{5h}) is maintained for both the equatorial and apical substitutions, leading to $ScSi_6$ (**6a**) and $ScSi_6$ (**6b**), respectively. The former is more stable than the latter by 0.598 eV. The framework of Si_7 (D_{5h}) is also retained for the equatorial substitution of Cu, yielding the substitutional structure $CuSi_6$ (**6b**), but the apical substitution of Cu induces reconstruction and results in an adsorption structure $CuSi_6$ (**6a**), in which the Cu atom is capped to a face of distorted Si_6 (C_{2v}-II) framework. These results justify the expectation based on charge analysis as mentioned above. $CuSi_6$ (**6a**) and $CuSi_6$ (**6b**) are nearly isoenergetic with an energy separation of only 0.078 eV, and they have both been reported in our previous contribution.[8]

In analogy to the observations made for smaller $ScSi_n$ clusters, we found that the Si_6 framework in $ScSi_6$ (**6a**) and $CuSi_6$ (**6a**, **6b**) can be more readily related to anionic Si_6^- (C_{2v}-II) than to neutral Si_6 (C_{2v}-II), suggesting again a charge transfer from Sc or Cu to the Si_6 framework. This agrees with the natural population analysis given in Table 3.

As indicated in previous publications,[7,8] endohedral $CuSi_6$ with Cu at the center (D_{4h} or O_h) is unstable and relaxes to the substitutional structure $CuSi_6$ (**6b**). A similar instability resulted from placing Sc at the center of Si_6 (D_{4h} or O_h), and the Sc atom relaxed to the surface, too. The reason is that the insertion of the metal atom impurity at the center site leads to a dramatic expansion of the Si_6 cage. As a consequence, the interaction between the Si ligand atoms vanishes almost completely. Therefore, the endohedral structure is unfavorable for both $CuSi_6$ and $ScSi_6$.

In two previous publications,[11,12] the substitution for the apical atoms of Si_7 (D_{5h}) was examined in $MoSi_6$ and WSi_6. The substitutional structures turned out to be stable with some distortion; they are the most stable isomers reported for these two clusters. For WSi_6, the substitution for the equatorial atoms of Si_7 (D_{5h}) was also considered, but the optimized geometry is strongly reconstructed, and it is less stable than the apical substitutional structure by 0.28 eV at the B3LYP/LanL2DZ level, showing a clear preference for the apical substitution. In addition, endohedral $TMSi_6$ (TM = Mo, W) was found to be stable with Si_6 in O_h symmetry but turned out to be of lesser stability than the apical substitutional structures by 1.19 and 0.14 eV, respectively, at the B3LYP/LanL2DZ level. The findings for $CrSi_6$ are similar to those for $MoSi_6$ and WSi_6. The octahedral center site structure is more stable than the equatorial substitutional structures for $TMSi_6$ (TM = Cr, Mo, W). All of these results suggest a complementarity of M (M = Cu, Sc) and TM (TM = Cr, Mo, W) with respect to the stabilities of endohedral and substitutional species, as predicted above on the basis of charge analysis.

The bonding characters in $ScSi_6$ (**6a**) and $CuSi_6$ (**6a** and **6b**) can be understood by their relations to Si_6 (C_{2v}-II) or Si_7 (D_{5h}). The β-HOMO and second α-HOMO of $ScSi_6$ (**6a**), as well as the α-HOMO of $CuSi_6$ (**6b**), all correspond to the LUMO of Si_6 (C_{2v}-II) or the HOMO of Si_7 (D_{5h}) (see Figure 2). They have components similar to those of Si_7 (D_{5h}) on the respective Si atoms, while the large p components on the 7Si atom of Si_7 (D_{5h}) is replaced by the large d and p components on the Sc atom of $ScSi_6$ (**6a**) or by the large p and considerable d components on the Cu atom of $CuSi_6$ (**6b**). Therefore, the strong bond between 7Si and the two neighboring equatorial atoms (3Si, 4Si) in Si_7 (D_{5h}) is imitated by the substitutional Sc atom in $ScSi_6$ (**5a**) or the Cu atom in $CuSi_6$ (**6b**). Regarding $CuSi_6$ (**6a**), the α-HOMO corresponds to the LUMO of Si_6 (C_{2v}-II) with little modification due to the presence of Cu.

The unpaired electron is located in the α-HOMO at $ScSi_6$ (**6a**) and $CuSi_6$ (**6a** and **6b**). It is essentially attached to the Sc atom in $ScSi_6$ (**6a**) but is spread over the equatorial atoms (3Si through 6Si) in $CuSi_6$ (**6a**, **6b**) (see Figure 3 and Table 3).

The natural charge and spin population analysis for atoms in all MSi_6 (M = Sc, Cu) clusters are listed in Table 3. Similar to the observations made for smaller clusters, the M atom loses charge to neighboring Si atoms in all MSi_6 isomers.

General Discussion. In summary, by placing an M atom (M = Sc, Cu) at various substitutional positions of Si_{n+1} ($n = 1-6$),

as well as adsorption positions of Si_n ($n = 2-4$) clusters and fully relaxing the resulting structures, we have determined possible low-lying isomers of MSi_n and examined the influence of the M atom on the structures and electronic properties of Si_n units.

The structures for the most stable isomers (***n*a**) of $ScSi_3$, $ScSi_5$, $CuSi_5$, and $ScSi_6$ are the substitutional ones, which leaves the frames of ground-state or low-lying isomers of Si_{n+1} nearly unchanged with Sc and Cu occupying various substitutional sites, while the lowest-energy structures for $ScSi_2$, $CuSi_2$, $CuSi_3$, $ScSi_4$, $CuSi_4$, and $CuSi_6$ belong to the adsorption type, in which Sc and Cu are capped on various surface sites of ground-state Si_n^-. For $CuSi_3$, $CuSi_4$, and $CuSi_6$, alternative candidates for the ground-state structures are found, which are the substitutional structures $CuSi_3$ (**3b)** and $CuSi_6$ (**6b**) and the adsorption structures $CuSi_3$ (**3c**) and $CuSi_4$ (**4b**, **4c**).

The charge transfer in MSi_n (M = Sc, Cu) is found to proceed from M to the adjacent Si atoms of Si_n framework in all clusters that we have considered and is stronger in $ScSi_n$ than in $CuSi_n$ (see Table 3). A similar charge transfer was found in $NaSi_n$ (from Na to Si_n) and Sc-encapsulating fullerenes (from Sc to C cage).[15,25,26] A charge-transfer proceeding in the opposite direction, from Si_n to TM, was recorded for $TMSi_n$ (TM = Cr, Mo, W).[10−12]

The opposing charge-transfer directions in MSi_n (M = Sc, Cu) and $TMSi_n$ (TM = Cr, Mo, W) are associated with opposite substitutional behaviors of M and TM in the substitutional structures based on Si_{n+1} ($n = 3-6$). Sc and Cu prefer to substitute for the Si atoms of Si_{n+1} that possess positive charges, which correspond to the atoms in the long diagonal (3Si, 4Si) of Si_4 rhombus or the equatorial atoms (3Si through 7Si) of Si_5 to Si_7, while Cr, Mo, and W prefer to substitute for the Si atoms of Si_{n+1} that adopt negative charges, which correspond to the atoms in the short diagonal (1Si, 2Si) of Si_4 rhombus or the apical atoms (1Si, 2Si) of Si_5 to Si_7.

The bonding properties for the most stable and nearly isoenergetic isomers of MSi_n (M = Sc, Cu) are understood by relating their HOMOs to the HOMOs or LUMOs or both of corresponding Si_n or Si_{n+1} clusters. The d orbitals of Sc have strong hybridization with the s and p orbitals of the Si atoms, showing a significantly delocalized character and active role in the Sc−Si bonding, while the d orbitals of Cu are much more localized, exhibiting only a small degree of hybridization with the orbitals of Si.

To illustrate these bonding features more clearly, we present the total and partial densities of states (DOS) for the representative $ScSi_6$ (**6a**) and $CuSi_6$ (**6b**) clusters in Figures 4 and 5, respectively. We chose these two isomers because they have similar substitutional structures and hence are suitable for comparison. The total DOS for a cluster is obtained by a Lorentzian broadening of the discrete energy levels of the cluster and a summation over them, while the partial DOSs are obtained by decomposing the total DOS into contributions due to various atomic orbitals, applying Mulliken population analysis. The broadening width is chosen to be 0.10 eV. From Figure 4, one notices that the Sc d orbitals contribute significantly to the four highest occupied peaks of the total DOS, spreading over a range from −1.0 to −3.0 eV below the Fermi level, and that there is strong hybridization between Sc d and Si s and p orbitals. In contrast, the Cu d orbitals are nearly localized at about 4.6 eV below the Fermi level and hence contribute little to the Cu−Si bonding. In addition to the d−sp hybridization between Sc and the Si atoms, there is also noticeable hybridization between the s and p orbitals of Sc or Cu and those of the Si atoms. Therefore,

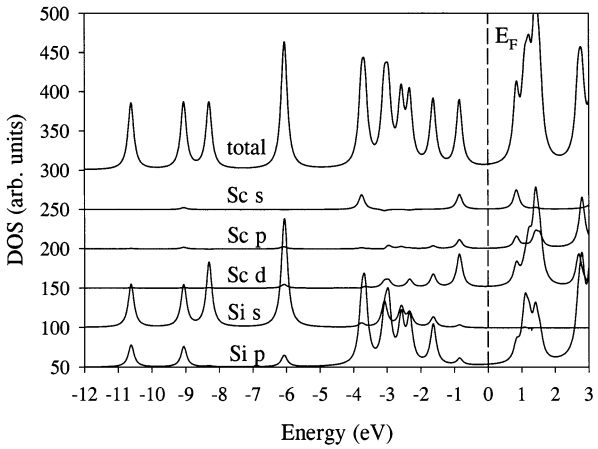

Figure 4. Total and partial densities of states (DOS) of the representative cluster $ScSi_6$ (**6a**). The energy is relative to the Fermi level (E_F).

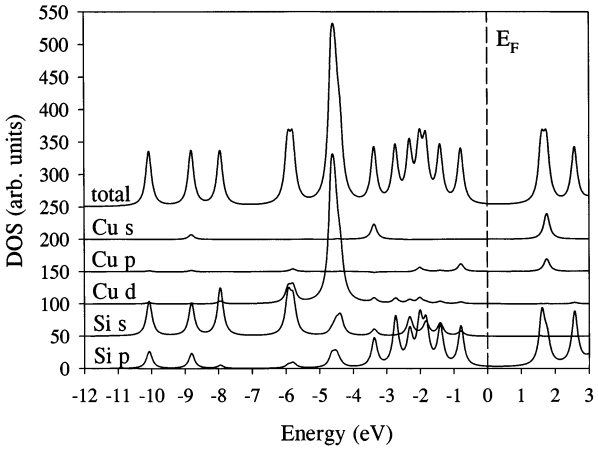

Figure 5. Total and partial densities of states (DOS) of the representative cluster $CuSi_6$ (**6b**). The energy is relative to the Fermi level (E_F).

a mixed ionic and covalent bonding picture between Sc or Cu and the Si atoms emerges in $ScSi_6$ (**6a**) and $CuSi_6$ (**6b**). Recently, evidence for the strong hybridization between the d orbitals of doped TM atoms and the cage orbitals was reported experimentally for $La@C_{82}$[27] and demonstrated in theoretical calculations for $TM@C_{60}$ and $TM@C_{82}$ with TM = La, Y, and Sc,[25,26] which is in contrast to the pure charge-transfer model for TM = La and Y and the d-electron localization model for TM = Sc that were proposed previously for these systems.

According to natural population analysis, the electronic configurations that we obtained for Sc in $ScSi_6$ (**6a**) and Cu in $CuSi_6$ (**6b**) are as follows: Sc $4s^{0.62}3d^{1.51}4p^{0.04}4d^{0.05}$ and Cu $4s^{0.41}3d^{9.89}4p^{0.05}$. Obviously, the 3d shell of Sc in $ScSi_6$ (**6a**) is open, and there is considerable charge transfer from Sc 4s to Sc 3d, as well as to Si s and p orbitals, leading to a strong hybridization between the s and d orbitals of Sc and the s and p orbitals of Si as shown in Figure 4. In contrast, the charge transfer in $CuSi_6$ (**6b**) takes place mainly from Cu s to Si s and p orbitals, while the 3d shell of Cu in the cluster remains nearly closed and thus contributes little to the Cu−Si bonding.

The DOSs and electronic configurations for M in all other MSi_n (M = Sc, Cu) isomers are quite similar to the two representative cases described above. In Figures 6 and 7, we present the partial DOSs for the M d orbitals in the most stable isomers of MSi_n. One can see that the M d orbitals for all clusters are located at similar positions below the Fermi level. With the increase of cluster size, the Sc d orbitals spread over an increasing range with the main peak shifted slowly upward

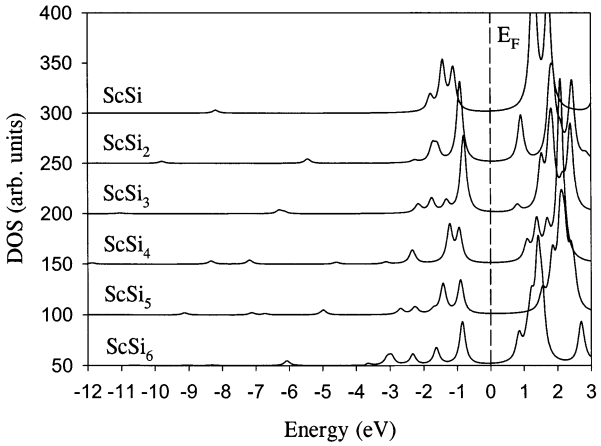

Figure 6. Partial densities of states (DOS) of Sc d orbitals in the most stable isomers of $ScSi_n$ ($n = 1-6$). The energy is relative to the Fermi level (E_F).

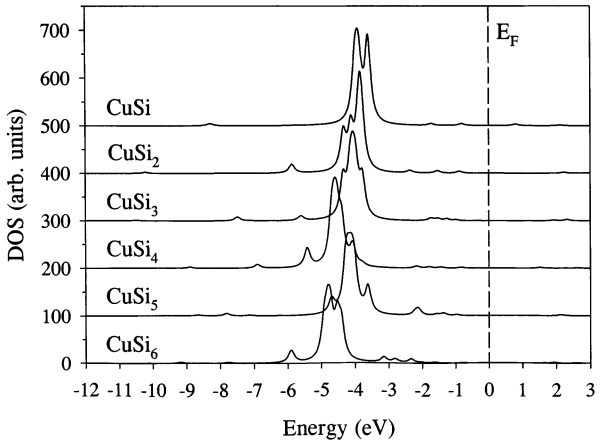

Figure 7. Partial densities of states (DOS) of Cu d orbitals in the most stable isomers of $CuSi_n$ ($n = 1-6$) clusters. The energy is relative to the Fermi level (E_F).

in energy, while the Cu d orbitals are localized in a much deeper position with the main peak shifted gradually downward in energy.

The spin polarization is localized on the Sc atom (**2a**, **3a**, **6a**) or shared by Sc and Si atoms (ScSi, **4a**, **5a**) in the most stable structures of $ScSi_n$ clusters. For $CuSi_n$, the Cu atom shows noticeable spin polarization only in $CuSi_3$ (**3a**) and $CuSi_4$ (**4a, 4b**), while the spin polarization in CuSi, $CuSi_2$ (**2a**), $CuSi_3$ (**3b**), $CuSi_4$ (**4c**), $CuSi_5$ (**5a**), and $CuSi_6$ (**6a, 6b**) is distributed among the Si atoms with little contribution from Cu (see Figure 3 and Table 3).

By examining all isomers of $ScSi_n$ and $CuSi_n$, we find that Sc has a stronger tendency to stabilize a substitutional structure than Cu. Substituting Sc for the Si atoms in both the long and short diagonals of rhombic Si_4 (D_{2h}) and for the Si atoms at both the equatorial and apical sites of Si_5 (D_{3h}) and Si_7 (D_{5h}) leads to stable substitutional structures (see Figure 1). The substitutions of Cu for the Si atoms in the short diagonal of Si_4 (D_{2h}) and for the Si atoms at the apical sites of Si_5 (D_{3h}) and Si_7 (D_{5h}) all result in dramatic reconstruction and relax into adsorption structures. A common feature of Si atoms in the short diagonal of Si_4 (D_{2h}) and of Si atoms at the apex sites of Si_5 (D_{3h}) and Si_7 (D_{5h}) is that they have a negative charge while the charge state of Cu in $CuSi_n$ is positive. For Sc, although the substitution for Si atoms in such negative-charge sites can be stable, they are of less stability than the substitution for Si atoms that carry positive charge. The principal reason for the lower stability of Cu-based substitutional structures is that the Cu−Si interaction is considerably weaker than the Sc−Si interaction in clusters except for their dimers, as will be discussed below.

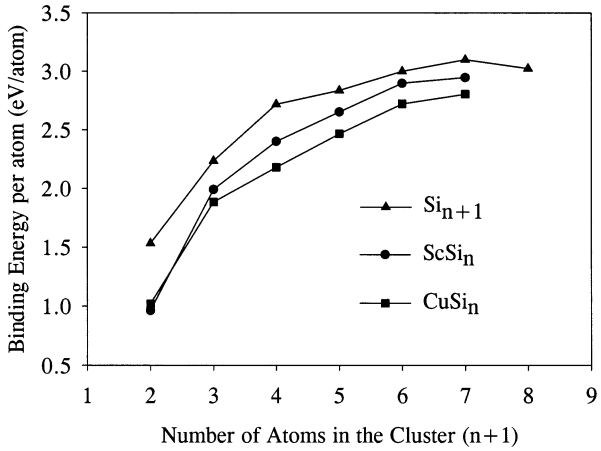

Figure 8. Size dependence of the binding energies per atom for the most stable isomers of MSi_n (M = Sc or Cu; $n = 1-6$) and Si_{n+1} ($n = 1-7$) clusters at the B3LYP/6-311+G(d) level.

3.2. Energetic Properties of $ScSi_n$ and $CuSi_n$. To further understand the effect of M (M = Sc or Cu) on the structures and properties of Si_n, we calculated various energetic properties for the most stable isomers (***n*a**) of MSi_n, including the binding energies per atom, the fragmentation energies with respect to the processes $MSi_n \rightarrow M + Si_n$ or $Si + MSi_{n-1}$, the vertical and adiabatic ionization potentials, and electron affinities, and compared these quantities with the corresponding values of pure Si_n or Si_{n+1} clusters. We expect that these data could be helpful for experimental studies to be conducted in the future.

The binding energies per atom (BEs) for the most stable isomers of MSi_n (M = Sc or Cu, $n = 1-6$) and Si_{n+1} ($n = 1-7$) with respect to isolated atoms are presented in Table 1, and their size dependences are shown in Figure 8. The BE curve for pure Si_n clusters agrees well with the one obtained by Raghavachari et al. at the MP4/6-31G* level,[20,21] in which the enhanced stabilities of Si_4 and Si_7 are reflected by slight local maxima. For MSi_n clusters, it seems that MSi_2 and MSi_5 have slightly enhanced stabilities. For all cluster sizes except the ScSi and CuSi dimers, the stabilities of MSi_n and Si_{n+1} are in the order of $Si_{n+1} > ScSi_n > CuSi_n$, indicating that, on an average, the Si−Si bond is stronger than the Sc−Si bond and the latter is stronger than the Cu−Si bond.

A more appropriate way of comparing the local stabilities of different sizes of MSi_n (M = Sc or Cu, $n = 1-6$) clusters and comparing the relative strength of Si−Si, Sc−Si, and Cu−Si interactions is the study of the fragmentation energies (FEs). The fragmentation of MSi_n into both $M + Si_n$ and $Si + MSi_{n-1}$ and of Si_{n+1} ($n = 1-7$) into $Si + Si_n$ are considered, and the FEs are listed in Table 2 and shown in Figure 9. The FE curve for pure Si_{n+1} clusters reveals a size dependence similar to that obtained by Raghavachari et al. at the MP4/6-31G* level,[21] which indicates a prominently enhanced stability at Si_4, Si_6, and Si_7. For MSi_n, with respect to the fragmentation into both $M + Si_n$ and $Si + MSi_{n-1}$, an enhanced stability appears at MSi_2 and MSi_5, in agreement with the BE profile. We thus predict that MSi_2 and MSi_5 could occur with high abundance in the mass spectrum.

Similar to the hierarchy established by the BEs, the FEs of MSi_n (M = Sc, Cu, Si) with respect to $M + Si_n$ follow the order of $Si_{n+1} > ScSi_n > CuSi_n$ (except ScSi and CuSi dimers),

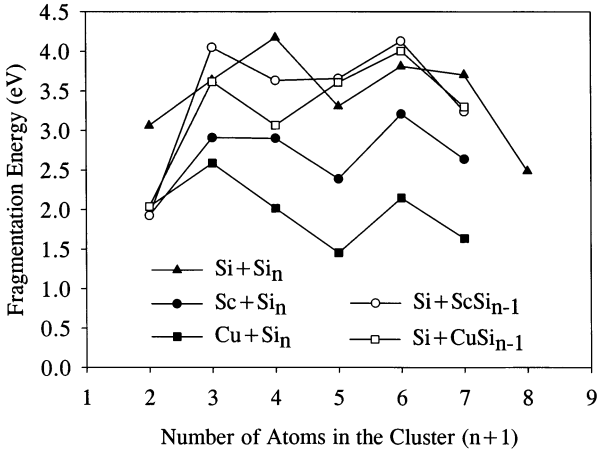

Figure 9. Size dependence of the fragmentation energies for the most stable isomers of MSi_n clusters with respect to $M + Si_n$ or $Si + MSi_{n-1}$ ($M = Sc$ or Cu; $n = 1-6$) at the B3LYP/6-311+G(d) level. For comparison, the fragmentation energies of Si_{n+1} with respect to $Si + Si_n$ ($n = 1-7$) at the B3LYP/6-311+G(d) level are also presented.

TABLE 4: Vertical and Adiabatic Ionization Potentials (VIP and AIP, in eV) and Electron Affinities (VEA and AEA, in eV) of the Most Stable Isomers of MSi_n ($M = Sc$, Cu; $n = 1-6$) and Si_n ($n = 1-7$) at the B3LYP/6-311+G(d) Level

cluster	VIP	AIP	VEA	AEA	cluster	VIP	AIP	VEA	AEA
ScSi	6.562	6.560	1.159	1.190	CuSi	7.246	7.246	1.473	1.475
$ScSi_2$	6.313	6.274	1.069	1.182	$CuSi_2$	7.436	7.375	2.103	2.115
$ScSi_3$	6.199	6.100	1.626	1.697	$CuSi_3$	7.781	7.109	2.266	2.771
$ScSi_4$	7.873	6.375	1.662	1.812	$CuSi_4$	7.108	6.968	2.053	2.365
$ScSi_5$	6.842	6.500	1.978	2.087	$CuSi_5$	7.621	7.007	2.290	2.689
$ScSi_6$	5.872	5.788	1.547	1.649	$CuSi_6$	6.911	6.680	2.094	2.308
Si	8.112	8.112	1.327	1.327	Si_2	7.922	7.919	2.046	2.091
Si_3	8.226	8.183	1.927	2.312	Si_4	8.096	7.882	2.086	2.103
Si_5	8.167	7.981	1.504	2.438	Si_6	7.952	7.561	1.360	2.207
Si_7	8.043	7.745	1.628	1.964					

indicating once again that the relative bonding strength of Si−Si, Sc−Si, and Cu−Si bonds is in the order of Si−Si > Sc−Si > Cu−Si.

The vertical and adiabatic ionization potentials (VIP and AIP) and electron affinities (VEA and AEA) for the most stable isomers of MSi_n ($M = Sc$, Cu; $n = 1-6$) are listed in Table 4, and their size dependences are plotted in Figures 10 and 11, respectively. For comparison, the vertical and adiabatic IPs and EAs for pure Si_n ($n = 1-7$) calculated at the B3LYP/6-311+G(d) level are also presented.

The size dependences of AIPs and AEAs that we obtained for pure Si_n clusters at the B3LYP/6-311+G(d) level agree well with those determined by Raghavachari et al.[23,24] at the MP4/6-31G* or MP3/6-31G* level and obtained by Wei et al.[28] using density functional calculation with the AIP curve showing an odd−even oscillation. The VIPs and AIPs of Si_n are similar in their size dependences, but the VEAs and AEAs of Si_n differ markedly for $N = 5-7$, reflecting the fact that the anionic species of these three clusters undergo significant relaxation.

For $CuSi_n$ clusters, the IPs and EAs show somewhat similar size dependences to the AIP and AEA curves for pure Si_n (see Figures10 and 11). These results are consistent with the fact that the HOMO and LUMO of $CuSi_n$ are dominated by the contributions from the orbitals of Si_n framework with little or minor contribution from the orbitals of Cu (see Figures 5 and 7). The noticeable differences between the VIPs and AIPs for $CuSi_3$ and $CuSi_5$ and between the VEAs and AEAs for $CuSi_3$ through $CuSi_5$ result from the considerable amount of reconstruction undergone by $CuSi_n$ in this size region upon ionization or addition of one electron.

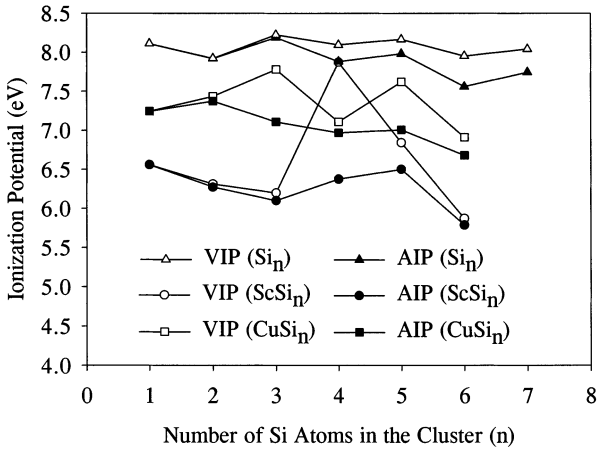

Figure 10. Size dependence of the vertical and adiabatic ionization potentials (VIP and AIP) for the most stable isomers of MSi_n ($M = Sc$ or Cu; $n = 1-6$) and Si_n ($n = 1-7$) clusters at the B3LYP/6-311+G(d) level.

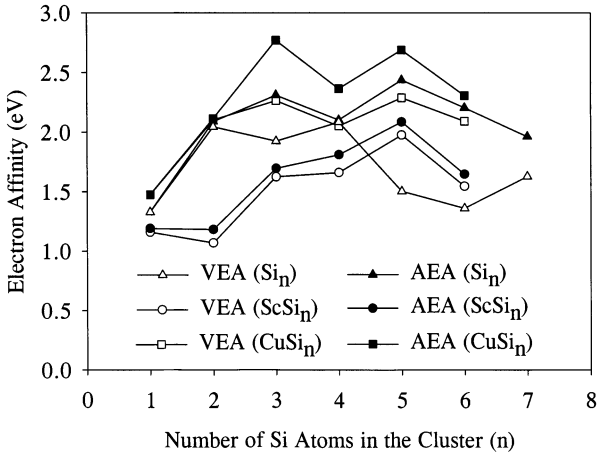

Figure 11. Size dependence of the vertical and adiabatic electron affinities (VEA and AEA) for the most stable isomers of MSi_n ($M = Sc$ or Cu; $n = 1-6$) and Si_n ($n = 1-7$) clusters at the B3LYP/6-311+G(d) level.

In contrast, neither the IPs nor the EAs for $ScSi_n$ clusters show any similarity in their size dependences to the corresponding curves of Si_n clusters, in keeping with the fact that the HOMO and LUMO of $ScSi_n$ have dominant or large contributions from the orbitals of Sc (see Figures 4 and 6). As compared with $CuSi_n$ clusters, $ScSi_n$ undergoes considerable reconstruction upon charging only for $ScSi_4^+$ and $ScSi_5^+$, in accordance with the enhanced stability of $ScSi_n$ as compared to $CuSi_n$.

Kishi et al.[15] and Wei et al.[28] have performed calculations on the structures and energetics of small $NaSi_n$ clusters with n up to 7 or 10 using ab initio or density functional methods, respectively. Both studies indicated that the most stable isomers of $NaSi_n$ retain the frames of Si_n nearly unchanged with the Na atom occupying various adsorption sites and that there is a charge transfer from Na to Si_n frameworks so that the Si_n frameworks and electronic structure of $NaSi_n$ correspond to those of Si_n^-. In addition, Wei et al.[26] found that $NaSi_2$ and $NaSi_5$ have an enhanced stability over the neighboring clusters with respect to the fragmentation into $Na + Si_n$. All of these results agree with our findings for MSi_n ($M = Sc$, Cu). However, Kishi et al.[15] and Wei et al.[28] also found that there exists a correlation in the size dependence between the IPs of $NaSi_n$ and the EAs of pure Si_n. Such correlation is not observed in the cases of MSi_n. This difference may be ascribed to the difference in the bonding mechanisms operative between metal and silicon atoms

in $NaSi_n$ and MSi_n, which is nearly pure ionic in the former but is a mixture of ionic and covalent interactions in the latter.

4. Conclusions

In this paper, a comparative study on the interaction of Sc and Cu atoms with small Si_n ($n = 1-6$) clusters was performed by means of a hybrid density functional technique (B3LYP) in combination with a 6-311+G(d) basis set. The substitutional effect of M (M = Sc, Cu) on Si_{n+1} framework was examined for all cluster sizes under study. In addition, the adsorption effect of M on Si_n framework was also considered for $n \leq 4$, and the possible existence of endohedral structures was examined for MSi_6.

With the exception of ScSi dimer, which is a spin quartet, the ground states for all isomers of MSi_n are spin doublets.

The structures for the most stable isomers (***n*a**) of $ScSi_3$, $ScSi_5$, $CuSi_5$, and $ScSi_6$ are the substitutional ones, which maintain the frameworks of Si_{n+1} nearly unchanged with Sc and Cu occupying various substitutional sites, while the lowest structures of $ScSi_2$, $CuSi_2$, $CuSi_3$, $ScSi_4$, $CuSi_4$, and $CuSi_6$ belong to the adsorption type, in which the Sc and Cu atoms were found to be attached to various surface sites of Si_n. For $CuSi_3$, $CuSi_4$, and $CuSi_6$, competitive candidates for the ground-state structures were found, which can also be classified as substitutional (**3b**, **6b**) or adsorption (**3c**, **4b**, **4c**) type. The geometric configurations for the most stable isomers of $ScSi_n$ and $CuSi_n$ are similar only in their dimer and trimer ($n = 1, 2$) but are different in all other cluster sizes, implying different growth mechanisms for $ScSi_n$ and $CuSi_n$ clusters.

The charge transfer in all MSi_n clusters (M = Sc, Cu) was found to proceed from M to the Si_n framework and is stronger in $ScSi_n$ than in $CuSi_n$. This charge-transfer behavior is similar to that detected in $NaSi_n$ (from Na to Si_n) and in Sc-encapsulating fullerenes (from Sc to C cage,[15,25−27] but opposite to the case of $TMSi_n$ with TM = Cr, Mo, W (from Si_n to TM).[10−12]

The opposite directions of charge-transfer behaviors between metal and silicon in MSi_n and $TMSi_n$ are found to be related to different substitutional patterns of M and TM atoms for Si atoms in Si_{n+1}. The M atoms prefer to substitute for the positively charged Si atoms of Si_{n+1}, while the TM atoms favor the Si sites of negative charge. As a result, the most stable structures of MSi_n are usually different from those of $TMSi_n$. In addition, an endohedral structure was found to be stable for $TMSi_6$, but such structures turn out to be unstable for MSi_n because they relax to adsorption geometries with M occupying a surface site.

The bonding properties for the most stable isomers of MSi_n (M = Sc, Cu) were explained by analyzing their relations to the corresponding Si_n or Si_{n+1} clusters and by inspection of the total and partial densities of states. The Sc d orbitals in $ScSi_n$ were found to contribute strongly to the orbitals around the Fermi level of the cluster and hybridize strongly with the s and p orbitals of Si atoms. In contrast, the d shell of Cu in $CuSi_n$ remains nearly closed, being localized at about 4.6 eV below the Fermi level, and contributes little to the Cu−Si bonding. In addition, noticeable hybridization between the s and p orbitals of Sc and Cu with the s and p orbitals of Si atoms in MSi_n clusters was observed. Therefore, a mixed ionic and covalent bonding picture between M and Si atoms emerges in MSi_n. This bonding picture is in contrast to the nearly pure ionic interaction between Na and Si atoms in $NaSi_n$ but consistent with recent experimental and theoretical findings on the existence of strong hybridization between TM d and cage orbitals in $TM@C_{60}$ and $TM@C_{82}$ (TM = La, Y, Sc).[25−27]

Because both the charge transfer and the hybridization between the metal and silicon orbitals are considerably larger in $ScSi_n$ than in $CuSi_n$, the Sc−Si interaction is generally stronger than the Cu−Si interaction and more substitutional structures were identified as stable for $ScSi_n$ than for $CuSi_n$.

The unpaired electron was found to be localized on the Sc atom or shared by Sc and Si_n framework in $ScSi_n$ clusters, but it is situated on Si_n in $CuSi_n$ with small or little contribution from Cu. This is in agreement with the strong Sc−Si hybridization in $ScSi_n$ and the weak Cu−Si hybridization in $CuSi_n$.

On the basis of the optimized structures, various energetic properties were calculated for the most stable isomers of MSi_n, including the binding energies per atom, the fragmentation energies with respect to M + Si_n or Si + MSi_{n-1}, the vertical and adiabatic ionization potentials, and electron affinities. These quantities were compared with the corresponding values of pure Si_n or Si_{n+1} clusters.

The size dependence of the binding and fragmentation energies consistently indicate that there is enhanced stability for MSi_2 and MSi_5, which agrees with the theoretical finding of enhanced stability at $NaSi_2$ and $NaSi_5$ in $NaSi_n$ clusters.[28] Therefore, we expect that MSi_2 and MSi_5 could be produced with high relative abundance in the mass spectrum.

Finally, good correlation between the size dependence of IPs for $NaSi_n$ and the EAs for Si_n is reported.[15,28] Such correlation, however, was not observed for MSi_n. This may be ascribed to the difference between the bonding principles governing $NaSi_n$ and MSi_n.

Acknowledgment. This work is supported by the National Science Foundation (NSF) through the CREST program under Grant HRD-9805465.

Supporting Information Available: The relative energies (in eV), electronic states, and optimized geometric parameters (in Å and deg) for all structures of Si_{n+1} and MSi_n (M = Sc, Cu; $n = 1-6$) clusters at the B3LYP/6-311+G(d) level. This material is available free of charge via the Internet at http://pubs.acs.org.

References and Notes

(1) Istratov, A. A.; Weber, E. R. *Appl. Phys. A* **1998**, *66*, 123.
(2) Fazio, A.; Caldas, M. J.; Zunger, A. *Phys. Rev. B* **1985**, *32*, 934.
(3) Beck, S. M. *J. Chem. Phys.* **1989**, *90*, 6306.
(4) Scherer, J. J.; Paul, J. B.; Collier, C. P.; Saykally, R. J. *J. Chem. Phys.* **1995**, *102*, 5190.
(5) Hiura, H.; Miyazaki, T.; Kanayama, T. *Phys. Rev. Lett.* **2001**, *86*, 1733.
(6) Xiao, C.; Hagelberg, F. *J. Mol. Struct. (THEOCHEM)* **2000**, *529*, 241.
(7) Xiao, C.; Hagelberg, F.; Ovcharenko, I.; Lester, W. A., Jr. *J. Mol. Struct. (THEOCHEM)* **2001**, *549*, 181.
(8) Xiao, C.; Hagelberg, F.; Lester, W. A., Jr. *Phys. Rev. B*, in press.
(9) Han, J. G.; Shi, Y. Y. *Chem. Phys.* **2001**, *266*, 33.
(10) Han, J. G.; Hagelberg, F. *Chem. Phys.* **2001**, *263*, 255.
(11) Han, J. G.; Hagelberg, F. *J. Mol. Struct. (THEOCHEM)* **2001**, *549*, 165.
(12) Han, J. G.; Xiao, C.; Hagelberg, F. *Struct. Chem.* **2002**, *13*, 175.
(13) Kumar, V.; Kawazoe, Y. *Phys. Rev. Lett.* **2001**, *87*, 45503.
(14) Kumar, V.; Kawazoe, Y. *Phys. Rev. B* **2002**, *65*, 73404.
(15) Kishi, R.; Iwata, S.; Nakajima, A.; Kaya, K. *J. Chem. Phys.* **1997**, *107*, 3056.
(16) Takata, M.; Umeda, B.; Nishibori, E.; Sakata, M.; Saito, Y.; Ohno, M.; Shinohara, H. *Nature (London)* **1995**, *377*, 46.
(17) Takata, M.; Nishibori, E.; Umeda, B.; Sakata, M.; Yamamoto, E.; Shinohara, H. *Phys. Rev. Lett.* **1997**, *78*, 3330.
(18) Frisch, M. J.; Trucks, G. W.; Schlegel, H. B.; Scuseria, G. E.; Robb, M. A.; Cheeseman, J. R.; Zakrzewski, V. G.; Montgomery, J. A., Jr.; Stratmann, R. E.; Burant, J. C.; Dapprich, S.; Millam, J. M.; Daniels, A. D.; Kudin, K. N.; Strain, M. C.; Farkas, O.; Tomasi, J.; Barone, V.; Cossi, M.; Cammi, R.; Mennucci, B.; Pomelli, C.; Adamo, C.; Clifford, S.;

Ochterski, J.; Petersson, G. A.; Ayala, P. Y.; Cui, Q.; Morokuma, K.; Malick, D. K.; Rabuck, A. D.; Raghavachari, K.; Foresman, J. B.; Cioslowski, J.; Ortiz, J. V.; Stefanov, B. B.; Liu, G.; Liashenko, A.; Piskorz, P.; Komaromi, I.; Gomperts, R.; Martin, R. L.; Fox, D. J.; Keith, T.; Al-Laham, M. A.; Peng, C. Y.; Nanayakkara, A.; Gonzalez, C.; Challacombe, M.; Gill, P. M. W.; Johnson, B. G.; Chen, W.; Wong, M. W.; Andres, J. L.; Head-Gordon, M.; Replogle, E. S.; Pople, J. A. *Gaussian 98*, revision A.9; Gaussian, Inc.: Pittsburgh, PA, 1998.

(19) Moore, C. E. *Atomic Energy Levels*; National Bureau of Standards Circular No. 467; National Bureau of Standards and Technology: Gaithersburg, MD, 1949.

(20) Raghavachari, K. *J. Chem. Phys.* **1986**, *84*, 5672.

(21) Raghavachari, K.; Rohlfing, C. M. *J. Chem. Phys.* **1988**, *89*, 2219.

(22) Shvartsburg, A. A.; Liu, B.; Jarrold, M. F.; Ho, K. M. *J. Chem. Phys.* **2000**, *112*, 4517.

(23) Raghavachari, K.; Logovinsky, V. *Phys. Rev. Lett.* **1985**, *55*, 2853.

(24) Raghavachari, K.; Rohlfing, C. M. *J. Chem. Phys.* **1991**, *94*, 3670.

(25) Lu, J.; Zhang, X.; Zhao, X. *Chem. Phys. Lett.* **2000**, *332*, 51.

(26) Lu, J.; Zhang, X.; Zhao, X.; Nagase, S. *Chem. Phys. Lett.* **2000**, *332*, 219.

(27) Kessler, B.; Bringer, A.; Cramm, S.; Schlebusch, C.; Eberhardt, W.; Suzuki, S.; Achiba, Y.; Esch, F.; Barnaba, M.; Cocco, D. *Phys. Rev. Lett.* **1997**, *79*, 2289.

(28) Wei, S.; Barnett, R. N.; Landman, U. *Phys. Rev. B* **1997**, *55*, 7935.